

# Nanofabrication of Biomaterial, CNT and Organic Polymer Patterned Thinfilms using Piezoelectric Ink Jet Printing

J.L. Sumerel\*, L.F. Deravi\*\*, D. W. Wright\*\*\*

\*Fujifilm Dimatix, Santa Clara, CA, USA, [jsumerel@dimatix.com](mailto:jsumerel@dimatix.com)

\*\*Vanderbilt University, Nashville, TN, USA, [leila.f.deravi@vanderbilt.edu](mailto:leila.f.deravi@vanderbilt.edu)

\*\*\*Vanderbilt University, Nashville, TN, USA, [david.wright@vanderbilt.edu](mailto:david.wright@vanderbilt.edu)

## ABSTRACT

**In contrast to thermal ink jetting that uses heat to generate fluid drop ejection, MEMS-constructed piezoelectric ink jet printheads use a thin PZT slab bonded to a silicon diaphragm to generate acoustic energy that drives drop formation without heat. This novel, non-contact, and nondestructive printing process immobilizes a variety of functional materials while retaining activity. By formulating an ink and determining jetting parameters, drop on demand immobilization of a variety of functional materials can be established for one-sided deposition. We have formulated a variety of inks for the printing of nanomaterials including silver, DNA, peptides, proteins, dendrimers and carbon nanotubes using both direct inking and scaffold carriers for the immobilization of nucleic acids and antibodies. Functionality is retained after printing.**

**Keywords:** piezoelectric printing, carbon nanotubes, biomaterials, thinfilms, dendrimers

## 1 PIEZOELECTRIC DROP ON DEMAND PRINTING

The required heating process for thermal ink jet printing (300 °C) will damage thermally-sensitive materials, thereby limiting their use in devising functional devices. [1,2] In contrast, using piezoelectric ink jet printing, temperature sensitive, functional materials are deposited under ambient conditions. Piezoelectric printheads contain a lead zirconate titanate (PZT) piezoelectric ceramic, nozzles, and a fluid chamber. When a voltage is applied to the PZT, mechanical vibrations create acoustic waves that in turn force fluid out of the chamber through the nozzles.[3] Piezoelectric printheads are categorized based on the deformation mode of the PZT (e.g., squeeze mode, bend mode, push mode, or shear mode).[4] At FUJIFILM Dimatix, the MEMS fabrication method for printhead production was adopted to increase the precision and resolution of the deposited materials.[5] These silicon devices increase jet-to-jet uniformity and drop placement accuracy. The inertness of the silicon expands the operating ranges to allow higher chemical diversity and

fluid throughput expanding piezoelectric ink jet printing from the ability to print graphic inks to the realm of printing functional fluids required for functional devices.

With regards to the technological advances incorporated into the DMP from FUJIFILM Dimatix, a unique feature of this table-top printing system is the printhead itself. For the first time, FUJIFILM Dimatix is producing high performance MEMS printheads that are intended to have a limited lifetime, filled once by the user, and then discarded. The silicon chip that completes the disposable printhead consists of 16 individually addressable jets that generate drops. These nozzles are spaced 254  $\mu\text{m}$  apart, but actual drop spacing during printing is determined by the lateral resolution with tuned head angle. The ink jet printhead is powered by a piezoelectric unimorph, which is constructed in the plane of the wafer and consists of patterned PZT bonded to a silicon diaphragm.[4] The silicon chip is bonded to a molded liquid crystal polymer frame with an electrical interface. This construct is the jetting module portion of the printhead and snaps to the fluid module to complete the FUJIFILM Dimatix disposable cartridge (Figure 1).



Figure 1. FUJIFILM Dimatix disposable cartridge

The fluid module is fabricated with a flexible polypropylene reservoir and protective rigid polypropylene housing. The volume of the reservoir is small (1.5 mL) which limits the amount of expensive materials used. Fluid flows directly from the reservoir through a small column into the printhead in the plane of the wafer through a silicon acoustic terminator and then into a pumping chamber. The fluid then flows down a descender and out the nozzles perpendicular to the wafer plane. The silicon nozzle/air interface is coated with a proprietary non-wetting material to reduce wetting of low surface tension fluids and to

facilitate printhead maintenance. The effective diameter of the nozzle is 21.5  $\mu\text{m}$ ; this nozzle size is approximated to generate 10 pL drops. An important operating parameter of this device is the negligible void volume due to the direct fluid to printhead interface.

## 2 MATERIALS AND METHODS

### Printer

The DMP-2831 (FUJIFILM Dimatix, Santa Clara, CA) was used according to packaging instructions. The DMC-11610 (10 pL) and DMC-11601 (1 pL) cartridges were removed from their storage bags and after degassing, 1.5 mL of fluid was injected into the cartridge. The cartridge was manually placed into the DMP carriage. The Drop Watcher camera system was activated utilizing the Drop Manager software. The default cleaning cycle was repeated until pulsating fluid could be seen at the nozzle plate. The time of flight (TOF) of the  $\sim 10$  pL drops was recorded using a built in stroboscopic broad band white light emitting diode and a charge coupled device camera with a high resolution 4x magnification lens that has a spectral response of greater than 60% between 400 and 700 nm. The camera's field of view is approximately 1.2 x 1.6 mm. The strobe frequency was matched to the firing pulse frequency (1 kHz for this application), and the motion control software's built-in variable delay and drop refresh rates were employed for visualization.

### Fluids

Multiwalled carbon nanotubes (1 mg  $\text{ml}^{-1}$ , OD = 20-30 nm, wall thickness = 1-2 nm, length 0.5-2  $\mu\text{m}$ ; Sigma Aldrich, St. Louis, MO) were mixed in a 53% polypropylene glycol 400, 45% propylene carbonate solution containing 0.01% tetramethyl-5-decyne-4,6-diol, 2,4,7,9-propanol (Surfynol 104PA; Air Products, Allentown, PA), 1 mg  $\text{ml}^{-1}$  salmon sperm deoxyribonucleic acid (Invitrogen, Carlsbad, CA) and 1  $\mu\text{g ml}^{-1}$  4,6 diaminidino-2-phenyl indole (DAPI). The solution was sonicated in a water bath for 25 min at 37°C. After sonication, the mixture was filtered through a 0.22  $\mu\text{m}$  syringe-tip filter (Pall Life Sciences, Ann Arbor, MI). Two percent (2%) glycerol (Sigma Aldrich, St. Louis, MO) was added to a poly (3,4-ethylenedioxythiophene) poly(styrenesulfonate) (PEDOT/PSS) aqueous dispersion (H.C. Stark, Goslar, Germany). ANP Silverjet nanopaste (Advanced Nanoproducts, Chungcheonguk-do, Korea) and Cabot Inkjet Silver Conductor (Ag-Ij-G-100-S1, Albuquerque, NM) were used as packaged. Fluids were sonicated in a water bath in a Branson 1510 sonicator at room temperature using highest sonic level for 30 minutes. Fluids were degassed for 2 hours at 5 mbar pressure in a degassing chamber.

### Substrates

Clean glass wafers were purchased from VWR (VWR Scientific, West Chester, PA). Both Kapton® (Dupont, Wilmington, DE) and Teslin® synthetic thin films (PPG Industries, Pittsburg, PA) were kept clean after purchasing and cut into 8" by 11" sheets using laboratory

scissors that had been cleaned with 70% ethanol (Sigma-Aldrich, St. Louis, MO). Single-side polished 150 mm silicon 100 wafers were obtained from Silicon Quest International (Santa Clara, CA) and sputtered with 300 nm gold layer using an Au target and a converted TES sputterer.

### Contact Angle Measurements

Contact angle measurements were carried out using a VCA Optima XE (AST, Billerica, MA). 2  $\mu\text{L}$  samples were manually pipetted for the measurements. The sample position between the LED backlight and the computer-interfaced camera was adjusted for optimal height and focus and then video captured. The associated software fit the silhouette and calculated the contact angle.

### Annealing

After printing both ANP Silverjet nanopaste and Cabot Inkjet Silver Conductor, samples were placed in a clean Yamato DX400 (Santa Clara, CA) gravity convection oven and baked for 1 hour at 200°C.

### Light Microscopy

Fluids on glass substrates were imaged using a Axiovert 200 inverted microscope (Carl Zeiss Inc., Thornwood, NY) using a standard DAPI filter

### Scanning electron microscopy

Samples were dried and evacuated. Scanning electron micrographs were obtained using a Philips XL30 ESEM or a S4200 scanning electron microscope (Hitachi, Tokyo, Japan). Resolution was obtained based on operating voltage. Operating voltage employed was 5 kV. Samples were magnified at either 20x or 80x.

### Atomic Force Microscopy

Tapping mode AFM was conducted on a Digital Instruments Dimension 3100 using an etched silicon tip with a nominal radius of curvature of 10 – 20 nm. Scan sizes were varied, depending on the feature size. The scan rate was 0.1 - 0.3 Hz. The set point was set to 60 - 70% of the free-standing root mean square of the voltage of the oscillating tip.

### Resistance Measurements

Resistance measurements were obtained using a Fluke 110 True RM multimeter. The anode was put at one end of silver contact on glass wafer and cathode was placed on top of other end of silver contact. Electrodes were manually held during measurements.

### Crystal Quartz Microbalance

Crystal quartz microbalance measurements of a 289 drop array were made using a research quartz crystal microbalance (Maxtek Inc., Beaverton, OR) and 9 MHz quartz crystals with chromium/gold electrodes. Baseline and adsorption frequency and resistance measurements were made after the electronics and the crystal were equilibrated. Resistance measurements were used to compensate for the density and viscosity effects of the contact solution. Frequency was converted to mass according to the Sauerbrey equation and previously known sensitivity factor (527 Hz/ $\mu\text{g}$ ).

### 3 RESULTS

We have formulated a variety of inks for the printing of nanomaterials including silver, DNA, peptides, proteins, dendrimers and carbon nanotubes using both direct inking and scaffold carriers for the immobilization of nucleic acids and antibodies.

Reliable printing procedures were established for two commercially available conductive silver precursors. Both fluids had ideal fluid flow properties for ink jet printing, and both fluids have higher than 50% silver nanoparticle load. The viscosity and surface tension values of the ANP Silverjet nanopaste are 9 cps and  $26.5 \text{ dynes cm}^{-1}$  respectively. Because of its high particle load (54%) and uniform particle size, low-temperature annealing produces traceable conductivity in the printed material. A screen capture of the jetting waveform is shown (Figure 2). This fluid jetted at a maximum frequency of 5.0 kHz with a pulse width of  $13.2 \mu\text{s}$ . The pulse peaked at maximum voltage after  $4.9 \mu\text{s}$  and was held for  $4.3 \mu\text{s}$ . It then recovered with a sharp  $0.3 \mu\text{s}$  slope to 25% maximum voltage. This voltage was held for  $0.3 \mu\text{s}$  and then was followed by an increase in voltage to 65% maximum voltage in  $0.3 \mu\text{s}$  and held for  $3.2 \mu\text{s}$ . The wavelength then sharply decreased to zero volts in  $0.9 \mu\text{s}$  and was held for  $3.7 \mu\text{s}$ . In general, it is found that each fluid has to be tuned with regards to waveform, voltage and frequency.

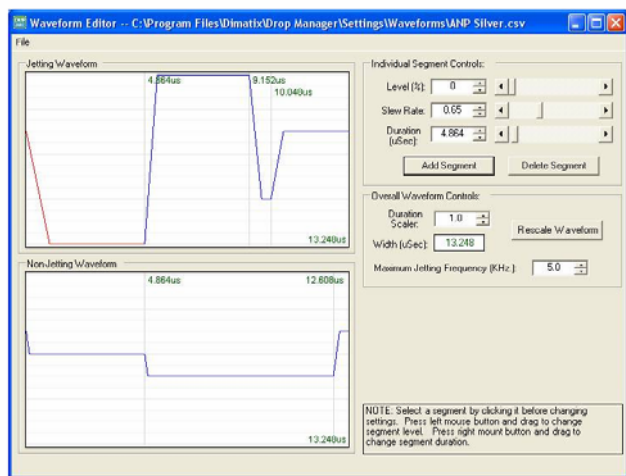


Figure 2. Jetting waveform for ANP Silverjet nanopaste.

Contact angle measurements demonstrate that ANP Silverjet nanopaste spreads on Kapton®, glass and Teslin with contact angles of  $14.9^\circ$ ;  $9.5^\circ$ , and  $40.25^\circ$  respectively (data not shown). These contact angles have established resulting feature resolution. After printing the nanopaste onto Teslin®, the printed material was annealed. Scanning electron micrographs were obtained to compare the films produced (Figure 3).

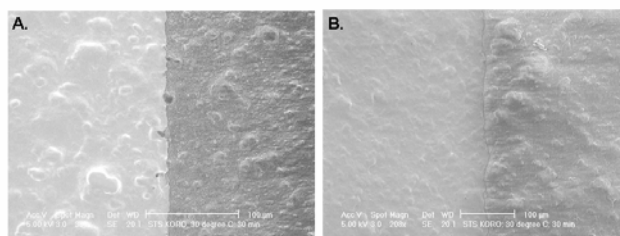


Figure 3. Scanning electron micrographs of ANP Silverjet nanopaste on Teslin. Panel A. Before annealing. Panel B. After annealing.

Panel A shows the ANP Silverjet nanopaste on Teslin® before annealing (silver on left, Teslin® on right). With single-pass printing, the fluid makes a uniform film on the Teslin® substrate in spite of the material's surface roughness (Panel A). Figure 10, panel B shows the same film on the same substrate after annealing for 1 hour at  $200^\circ\text{C}$  (annealed silver on left, Teslin® on right). Not only do the edges look slightly more uniform, but full coverage of the film on the substrate with single pass printing created a full coverage thin silver thin on the Teslin®. Because accurate feature measurements are difficult on flexible substrates, feature thickness was measured on gold-coated polished silicon nitride wafers (contact angle  $41.80^\circ$ , data not shown). We measured feature sizes using atomic force microscopy (AFM) with features printed at  $20 \mu\text{m}$  drop spacing (Figure 4) demonstrating that the feature size of a

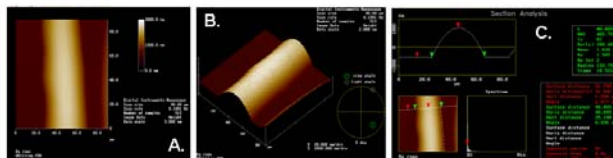


Figure 4. AFM of ANP Silverjet nanopaste.

single row of drops was uniform (Figure 4, panel A). The three-dimensional rendered view in Panel B shows the overall jetting uniformity. Panel C shows the calculated feature measurements. The width of the feature was  $40.6 \mu\text{m}$ , and the film thickness of  $1.59 \mu\text{m}$  demonstrates the utility of producing patterned thin films using ink jet printing technology. Because electrical performance is often described in terms of the bulk resistivity, resistance values were measured after annealing the silver nanoparticles (Figure 5).



Figure 5. Resistance measurements of two silver fluids

The resistance of the ANP Silverjet nanopaste is shown in Panel A (1.1 $\Omega$ ), and the resistance of the Cabot Inkjet Silver Conductor is shown in Panel B (0.3 $\Omega$ ). The low resistance measurements in both cases were taken on equally sized patterns on identical glass wafers. These values are in the same range as resistance values obtained by Sawhney and colleagues.[6]

Ink jet printing of hybrid composite containing multi-walled carbon nanotubes and deoxyribonucleic acid was also demonstrated. During these studies, the voltage to the nozzle was maintained at 27 V. Average drop size onto a gold surface was 98.4  $\mu\text{m}$  (standard deviation=5.4  $\mu\text{m}$ ). In Figure 6, the bright field micrograph of a single drop of the hybrid composite (Figure 6a) is compared to the DAPI staining (Figure 6b).

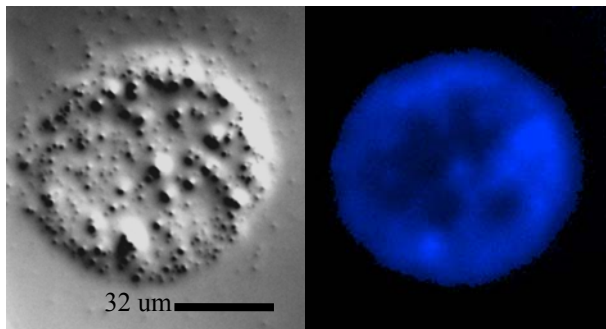


Figure 6. Optical micrograph of CNT/DNA hybrid composite.

It was shown that the 289 single drop array provided a mass of 861 ng (a mass per drop of 2.978 ng; data not shown). This printing process was greatly simplified by the ability of the Materials Deposition Printer to manipulate the waveform and voltage to an individual nozzle.

Characterization of other films will be discussed including ink jet printed dendrimers. After dendrimeric printing, patterned silicon dioxide thin films are grown on the material measuring less than 170 nm. We have demonstrated the strength and utility of this technique to print electronic components, and further directions will be to integrate these additive processes and couple them to device manufacturing.

## REFERENCES

- [1] Calvert, P., *Ink jet printing for materials and devices*. Chem. Mater. , 2001. 13: p. 3299-3305.
- [2] Xu, T., *Inkjet printing of viable mammalian cells*. Biomaterials, 2005. 26(1): p. 93-9.
- [3] Brünahl, J. and A.M. Grishij, *Piezoelectric shear mode drop-on-demand ink jet actuator*. Sens. Act. A, 2002. 101: p. 371-382.
- [4] Myatt, C., N. Traggis, and K.L. Dessau, *Optical fabrication: optical contacting grows more robust*. Laser Focus World, 2006. 42: p. 95-98.

- [5] Menzel, C. MEMS solutions for precision micro-fluidic dispensing application. in NIP20: International Conference on Digital Printing Technologies. 2005. Salt Lake City Utah.
- [6] Sawhney, A., et al., *Piezoresistive sensors on textiles by inkjet printing and electroless plating*. Mater. Res. Symp. Proc., 2006. 920: p. 4-13